Noise-Induced Coherence and Network Oscillations in a Reduced Bursting Model [3]

Conrad Foo, Myron Liu*
Physics Department, University of California San Diego

(Dated: December 10, 2013)

The Hindmarsh-Rose (HR) model is a popular choice for describing bursting neurons. Yet, it has the disadvantage of being quite complicated; for instance, it involves non-linear terms. It has been demonstrated that a much simpler Resonant Integrate-and-Fire (RIF) model can replicate much of the essential behaviour of the HR model. Of particular interest is the coherent resonant (CR) bursting pattern that emerges when neurons—more specifically networks of neurons—are subjected to noise. This topic has been addressed using stochastic methods.

I. RESONANT INTEGRATE-AND-FIRE MODEL

The RIF model is a simple model for neuron activity that closely matches the behaviour of the HR model (the details of which we shall not dive into). In the RIF model, the neuron is treated as a capacitor; the membrane is the dielectric preventing charge from flowing into or out of the neuron. One plate of the capacitor is the inside of the neuron and the other is comprised of the surrounding fluid. From classical electromagnetism, the voltage across the membrane (capacitor), is then $V(t) = Q(t)/Cap$. Taking the time-derivative of this equation gives:

$$\frac{dV}{dt} = \frac{1}{Cap}\frac{dQ}{dt}$$

Henceforth we shall set $Cap = 1$ so that $V = Q \equiv x$ The flux of charge through the membrane dx/dt has several constituents. First, the membrane is semi-permeable, and there is a leakage current proportional to the interior voltage (Ax). In addition, there is the external "source" current that is applied to the neuron (I_{signal}).

Finally, the model assumes that there are ion channels that open and close depending on the membrane potential. These channels add an additional term to the current through the membrane By, where y is a measure of the number of channels open (or the average "openness" of each channel). Since the channels open and close depending on the membrane potential, we expect that there should be a term proportional to the voltage V when writing dy/dt. Open channels also slowly relax to the closed position over time, providing a term Dy to dy/dt. Thus, the dynamical equation for the channel openness is:

$$\frac{dx}{dt} = Ax + By + I_{signal}(t) \quad (1)$$

$$\frac{dy}{dt} = Cx + Dy \quad (2)$$

To model the action potentials that are characteristic of neuron activity, a threshold value of the membrane potential is set, such that the membrane potential resets to its equilibrium value when the threshold is reached. In addition, a large number of ion channels open when the threshold potential is reached, as the electric field across the ion channels is large enough to change the conformation of most channels from closed to open. Therefore, whenever the threshold voltage is reached, a number y_{reset} is added to the current number of open channels y. The resulting coupled ODE system to describe a neuron is thus:

$$\frac{dx}{dt} = Ax + By + I_{signal}(t) \quad (3)$$

$$\frac{dy}{dt} = Cx + Dy \quad (4)$$

while in the sub-threshold regime. And when $x(t)$ exceeds x_{thresh}

$$x \to x_{reset}$$
$$y \to y + y_{reset}$$

To match the parameters A, B, C, D to the well-established (and more complex) HR model of neuron dynamics, the complex impedance of the membrane potential was found for a sinusoidal external current $\delta e^{i\omega t}$. Minimizing the difference between the magnitude of the impedance and that of the HR model (whose parameters have already been fixed via experiment) as a function of $\omega \equiv 2\pi/\lambda$, suitable parameters were found to be:

$$A = -0.032, B = -1.3258, C = 0.00025, D = -0.001$$

Figure 1 demonstrates that for such periodic $I_{signal}(t)$, RIF mimics HR accurately for a large spectrum of frequencies.

To develop an intuition for the RIF model, we first investigate its behaviour for constant positive input current. For instance, setting $I_{signal} = 0.4$ results in the traces shown in Figure 2. To summarize, x increases until x_{thresh} is reached, at which point, x is instantaneously set to x_{reset}. Meanwhile, y decreases exponentially, then jumps up by y_{reset} when the threshold is reached. In fact, x continues to decrease (and

*Electronic address: conradfoo@gmail.com, myronyliu@gmail.com

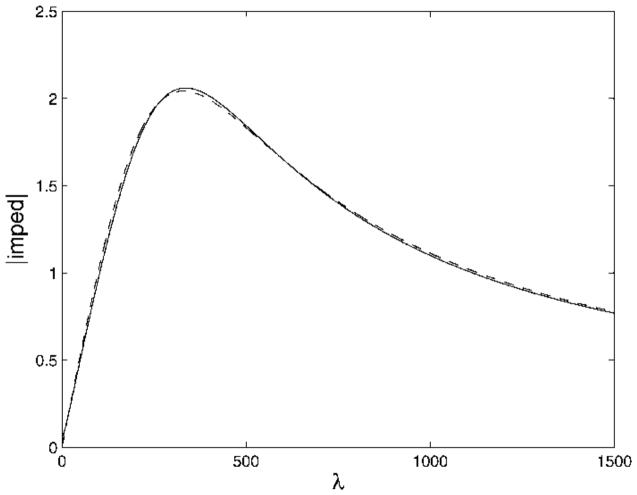

FIG. 1: In both the HR model and the RIF model, a neuron subjected to periodic input $I_{signal}(t) = \delta e^{i\omega t}$ undergoes oscillations in its membrane voltage. Namely, $x(t) = x_0(\omega)e^{i\omega t}$ where $x_0(\omega) \in \mathbb{C}$. For appropriate choice of parameters A, B, C, D, the magnitude of the impedance, defined as x_0/δ, nearly coincides for both models over a large swath of $\omega \equiv 2\pi/\lambda$. This makes a convincing case for using the RIF model in place of the more detailed HR model. [3]

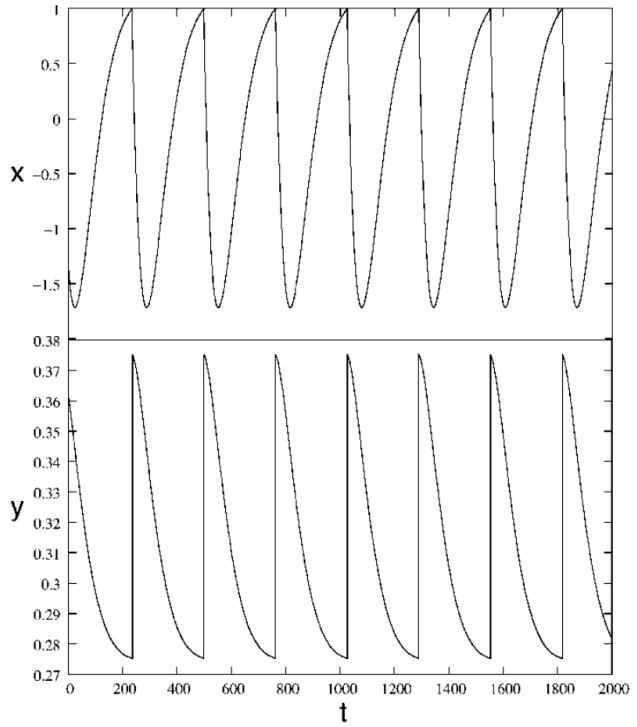

FIG. 2: $x(t)$ and $y(t)$ for $I_{signal} = 0.4$, $x_{thresh} = 1$, $x_{reset} = 0.9$, $y_{reset} = 0.1$ demonstrating the bursting behaviour of the RIF model. [3]

polarize in the opposite direction) after reset because y decays sufficiently slowly (*i.e.* the channels do not close fast enough)—recall that $B < 0$, so y suppresses dx/dt towards negative values. This is observed experimentally as hyper-polarization.

Note: In providing this qualitative description (and in producing Figure 2) we have used the fact that $|A| \ll |B|$ and the fact that $|C|$ is appreciably smaller than $|D|$ to eliminate Ax and Cx. Of course, among other things, the precise behaviour of $y(t)$ is not exponential decay, but it's a decent approximation.

In fact, although the original analysis was done as such (and with great success), we found the general approach of dropping the smaller terms questionable; it only provides a fraction of the whole story. The primary reason that doing so works here is that x_{thresh} was chosen to be sufficiently small.

First and foremost, let's solve the Equations 3 and 4 analytically for $I_{signal} = constant$. Without going into gory detail:

$$\begin{cases} \dot{x} = Ax + By + I_0 \\ \dot{y} = Cx + Dy \end{cases}$$

$$\Rightarrow \begin{cases} \ddot{x} = (A+D)\dot{x} - \gamma x - DI_0 \\ \ddot{y} = (A+D)\dot{y} - \gamma y + CI_0 \end{cases}$$

$$\Rightarrow \begin{cases} x(t) = C_1 e^{\kappa_+ t} + C_2 e^{\kappa_- t} + \frac{D}{\gamma} I_0 \\ y(t) = C_3 e^{\kappa_+ t} + C_4 e^{\kappa_- t} - \frac{C}{\gamma} I_0 \end{cases}$$

where

$$\gamma \equiv AD - BC$$

$$\kappa_\pm = \frac{1}{2}\left((A+D) \pm \sqrt{(A-D)^2 + 4BC}\right)$$

$$C_1 = \frac{\kappa_- - A}{\kappa_- - \kappa_+}(x_0 + \frac{D}{\gamma} I_0) - \frac{B}{\kappa_- - \kappa_+}(y_0 - \frac{C}{\gamma} I_0)$$

$$C_4 = \frac{\kappa_- - A}{\kappa_- - \kappa_+}(y_0 - \frac{C}{\gamma} I_0) - \frac{\kappa_- - A}{\kappa_- - \kappa_+}\frac{\kappa_+ - A}{B}(x_0 + \frac{D}{\gamma} I_0)$$

$$C_2 = \frac{B}{\kappa_- - A} C_4$$

$$C_3 = \frac{\kappa_+ - A}{B} C_1$$

The problem here is that using the given parameter values for A, B, C, D the exponents $\kappa_\pm$ are complex. Therefore, $x(t)$ and $y(t)$ exhibit oscillatory behaviour, which has been completely ignored. Nonetheless, this oscillatory behaviour is swamped by the larger exponential growth/decay.

In addition, rather than approach x_{thresh} asymptotically, $x(t)$ eventually curves back down and decays to zero. It is fortunate that $x_{thresh} = 1.0$ is sufficiently small such that before the unadulterated solution for $x(t)$ has an opportunity to diverge from the $C = 0$ solution, the threshold is achieved.

II. STOCHASTIC INPUT CURRENT

In the subsequent discussion, we let $I_{signal}(t) = \eta(t)$ be Gaussian white noise. We shall see that this can lead to coherent resonance (CR); the effect becomes particularly dramatic when we couple the neuron to a *network* of neurons. The system is now described by the stochastic differential equation:

$$dx = (Ax + By)dt + \sigma dW \tag{5}$$
$$dy = (Cx + Dy)dt \tag{6}$$

with the usual *reset* rules.

Clearly the stochastic nature of dW allows x to sporadically exceed x_{thresh}. What is more interesting, however, is that this can lead to the repeated firing behaviour shown in Figure 3 Even changing the value of σ approximately preserves the periodicity. A histogram of the inter-spike intervals (Figure 4) shows that for a wide range of σ the average time between successive spikes is unchanged.

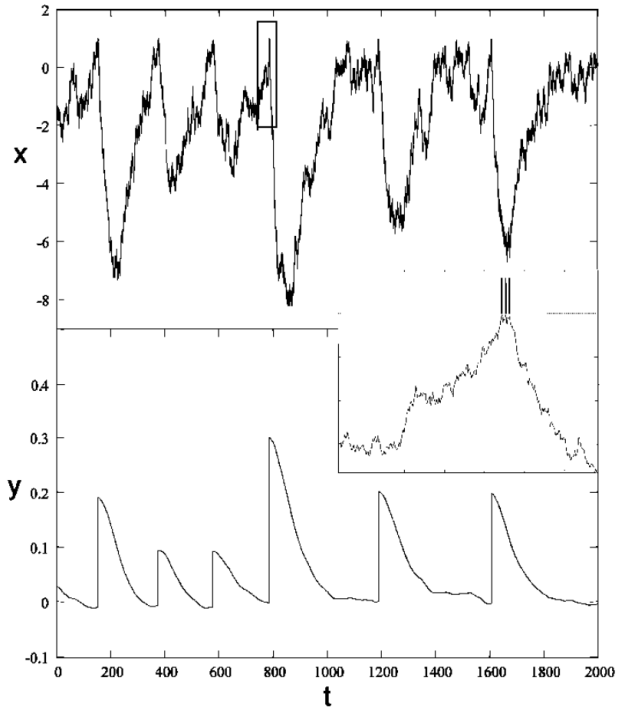

FIG. 3: For $\sigma = 0.2$, the neuron exhibits periodic firing). [3]

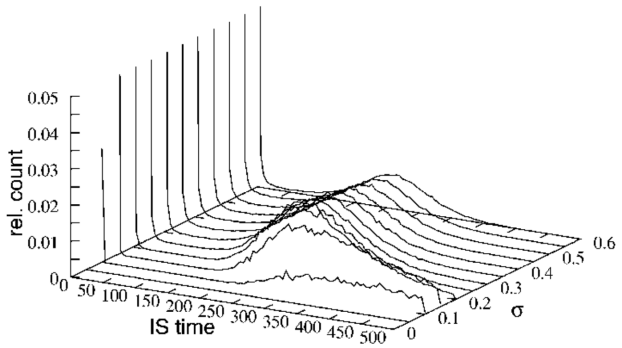

FIG. 4: Inter-spike interval histogram (ISIH) showing that the periodicity of neuron firing depends only weakly on the particular value of σ. The most densely occupied bin is always in the range of 200 to 300 time units, with slightly decreasing period for larger σ. The large spike near $t = 0$ is an artefact of choosing x_{reset} near x_{thresh}, which makes the neuron likely to fire repeatedly in a short span of time; which is what is shown in the magnified portion of Figure 3. Nonetheless, x will not linger at threshold; repeated crossings resets y to ever larger values so that x is inevitably suppressed. [3]

III. ANALYTICAL TREATMENT

From Equation 5 we can obtain a corresponding Fokker Planck Equation (FPE). Up to $\mathcal{O}(dt)$ the moments are:

$$\langle dx \rangle = (Ax + By)dt$$
$$\langle dx^2 \rangle = \sigma^2 dt$$
$$\langle dy \rangle = (Cx + Dy)dt$$

Here, we have used the fact that dW is a Weiner process to write $\langle dW^2 \rangle = dt$. The corresponding FPE is then:

$$\frac{\partial P}{\partial t} = -\frac{\partial}{\partial x}[(Ax + By)P] - \frac{\partial}{\partial y}[(Cx + Dy)P] + \frac{\sigma^2}{2}\frac{\partial^2 P}{\partial x^2} \tag{7}$$

where $P(x, y, t)$ is the probability density of finding the neuron in state (x, y) at time t.

Equation 7 describes a 2-component Ornstein-Uhlenbeck process. As in the lecture notes (chapter 2 and chapter 4), we can solve this equation by taking the spatial Fourier transform and applying the method of characteristics. The Fourier transform of the FPE is computed as follows. First, note that:

$$\begin{aligned}
\widehat{\partial_x(xP)} &= \int dxdy e^{-ik_x x} e^{-ik_y x} \partial_x(xP) \\
&= \int dxdy e^{-ik_x x} e^{-ik_y x}(P + x\partial_x P) \\
&= \widehat{P} + i\frac{\partial}{\partial k_x}\int dxdy e^{-ik_x x} e^{-ik_y x}\partial_x P \\
&= \widehat{P} + i\frac{\partial}{\partial k_x}(ik_x \widehat{P}) \\
\widehat{\partial_x(xP)} &= -k_x \frac{\partial \widehat{P}}{\partial k_x}
\end{aligned}$$

Similarly...

$$\begin{aligned}\widehat{\partial_x(yP)} &= \widehat{y\partial_x P} \\ &= \int dxdy e^{-ik_x x} e^{-ik_y x} y\partial_x P \\ &= i\frac{\partial}{\partial k_y}\int dxdy e^{-ik_x x} e^{-ik_y x}\partial_x P \\ &= i\frac{\partial}{\partial k_y}(ik_x\widehat{P}) \\ \widehat{\partial_x(yP)} &= -k_x\frac{\partial\widehat{P}}{\partial k_y}\end{aligned}$$

Using these two expressions, the Fourier transform of Equation 7 is:

$$\frac{\partial\widehat{P}}{\partial t} = (Ak_x + Ck_y)\frac{\partial\widehat{P}}{\partial k_x} + (Bk_x + Dk_y)\frac{\partial\widehat{P}}{\partial k_y} - \frac{\sigma^2}{2}k_x^2\widehat{P} \tag{8}$$

This is a quasi-linear PDE, and thus can be solved using the method of characteristics. The resulting solution in 1D is a Gaussian, as shown in the *PHYS210B* notes (chapter 2, appendix). To see that this is true in 2D as well, we turn the PDE into a set of coupled ODEs via the method of characteristics:

$$\begin{aligned}\frac{d\widehat{P}}{ds} &= \frac{\sigma^2 k_x^2}{2}\widehat{P} \\ \frac{dk_x}{ds} &= Ak_x + Ck_y \\ \frac{dk_y}{ds} &= Bk_x + Dk_y \\ \frac{dt}{ds} &= -1\end{aligned}$$

Note that the equations governing k_x and k_y are the same as the original coupled ODE system (equations 3 and 4) for a single neuron, with no I_{signal}. The solution for $\widehat{P}$ is then:

$$\begin{aligned}\widehat{P}(s) &= \widehat{P}(s=0)e^{\frac{\sigma^2}{2}\int_0^s ds' k_x^2(s')} \\ &= \widehat{P}(s=0)e^{\frac{\sigma^2}{2}\int_0^s ds'(C_1 e^{\kappa_+ s'} + C_2 e^{\kappa_- s'})^2}\end{aligned}$$

If the initial condition is assumed to be a delta function at $t=0$, then $\widehat{P}(s=0)$ can be written as:

$$\widehat{P}(s=0) = e^{-ik_x(s=0)x_0}e^{-ik_y(s=0)y_0} \tag{9}$$

From the solution to the constant current case, the coefficients C_1, C_2, C_3, and C_4 can be written in terms of $k_{x0} = k_x(s=0)$ and $k_{y0} = k_y(s=0)$. Plugging the expressions for these terms into the solutions for k_x and k_y and solving for k_{x0} and k_{y0} gives

$$\begin{aligned}k_{x0} =& \frac{(\kappa_- - A)k_x - Ck_y}{\kappa_+ - \kappa_-}e^{-\kappa_+ s} \\ &+ \frac{\kappa_- - D}{\kappa_+ - \kappa_-}e^{-\kappa_- s}(k_x - \frac{C}{\kappa_+ - A}k_y) \\ k_{y0} =& \frac{B}{\kappa_+ - \kappa_-}[(\frac{C}{\kappa_- - A}k_y - k_x)e^{-\kappa_+ s} \\ &+ (\frac{C}{\kappa_+ - A}k_y - k_x)e^{-\kappa_- s}]\end{aligned}$$

after some nasty algebra. We see that the initial condition 9 will be proportional to k_x and k_y, and represent the motion of the mean value of x and y, as the inverse Fourier transform will be an integral:

$$\int \frac{dk_x}{2\pi}\frac{dk_y}{2\pi}e^{ik_x(x - f(x_0,y_0,t)}e^{ik_y(y-g(x_0,y_0,t)}F[k_x,k_y,t]$$

In fact, substituting the expressions for k_{x0} and k_{y0} into equation 9 recovers the solution to the coupled ODEs 3 and 4 for $f(x_0,y_0,t)$ and $g(x_0,y_0,t)$. The C_n^2 terms in the exponential will be proportional to k_x^2, k_y^2, or k_xk_y. Thus, the exponential terms in the solution are of a general Gaussian form. Collecting terms and taking the inverse Fourier transform, we can read off the variances as a function of time by inspection:

$$\begin{aligned}\bar{x^2} &= \frac{\beta}{\alpha}^2 \\ \bar{y^2} &= \frac{\beta}{\gamma}^2 \\ \bar{xy}^2 &= \beta^2\end{aligned}$$

The parameters α, β, and γ are given by:

$$\begin{aligned}\beta =& \frac{\sigma^2}{4}\frac{(\kappa_+ - A)(\kappa_- - A)}{(\kappa_+ - \kappa_-)^2}[\frac{\kappa_- - A}{\kappa_+}(e^{2\kappa_+ t} - 1) \\ &+ \frac{\kappa_+ - a}{\kappa_-}(e^{2\kappa_- t} - 1) + \frac{2(\kappa_+ + \kappa_- - 2A)}{\kappa_+ + \kappa_-}(e^{(\kappa_+ + \kappa_-)t} - 1)] \\ \gamma^2 =& \frac{1}{2}\frac{\sigma^2}{(\kappa_+ - \kappa_-)^2}[\frac{(\kappa_- - A)^2}{2\kappa_+}(e^{2\kappa_+ t} - 1) \\ &+ \frac{(\kappa_+ - A)^2}{2\kappa_-}(e^{2\kappa_- t} - 1) \\ &+ \frac{2(\kappa_- - A)(\kappa_+ - A)}{\kappa_+ + \kappa_-}(e^{(\kappa_+ + \kappa_-)t} - 1)] \\ \alpha^2 =& \frac{\sigma^2}{2B^2}\frac{(\kappa_+ - A)^2(\kappa_- - A)^2}{(\kappa_+ - \kappa_-)^2}[\frac{2}{\kappa_+ + \kappa_-}(e^{(\kappa_+ + \kappa_-)t} - 1) \\ &+ \frac{e^{2\kappa_+ t} - 1}{2\kappa_+} + \frac{e^{2\kappa_- t} - 1}{2\kappa_-}]\end{aligned}$$

As the Fourier transform of a Gaussian is a Gaussian, $P(\vec{x},t)$ is also normally distributed. Knowing this, the equations governing the time evolution of the moments of the distribution are easily derived by making

use of the FPE. For demonstrative purposes, we compute $d\overline{x}/dt$. Integrating both sides of Equation 7 by $\int dxdyx$,

$$\begin{aligned}\int dxdyx\frac{\partial P}{\partial t} =& -\int dxdyx\frac{\partial}{\partial x}[(Ax+By)P]\\ &-\int dxdyx\frac{\partial}{\partial y}[(Cx+Dy)P]\\ &+\frac{\sigma^2}{2}\int dxdyx\frac{\partial^2 P}{\partial x^2}\end{aligned}$$

The left hand expression is just $d\overline{x}/dt$. Integrating by parts,

$$\begin{aligned}\frac{d\overline{x}}{dt} =& \int dxdy(Ax+By)P - \int dy\,[x(Ax+By)P]_{x=-\infty}^{+\infty}\\ &-\int dx\,[x(Cx+Dy)P]_{y=-\infty}^{+\infty}\\ &+\frac{\sigma^2}{2}\int dy\left[x\frac{\partial P}{\partial x}\right]_{x=-\infty}^{+\infty} - \frac{\sigma^2}{2}\int dy\,[P]_{x=-\infty}^{+\infty}\end{aligned}$$

All boundary terms vanish since P decays faster than any power of x, y. Then we are left with:

$$\frac{d\overline{x}}{dt} = A\overline{x} + B\overline{y}$$

We can perform the same sort of computation for other moments. As P is normally distributed, it suffices to compute the dynamical equations for $\overline{x}$, $\overline{y}$, $\overline{x^2}$, $\overline{xy}$, $\overline{y^2}$ to fix P. The time evolution of the moments is given by:

$$\begin{aligned}\frac{d\overline{x}}{dt} &= A\overline{x} + B\overline{y}\\ \frac{d\overline{y}}{dt} &= C\overline{x} + D\overline{y}\\ \frac{d\overline{x^2}}{dt} &= 2A\overline{x^2} + 2B\overline{xy} + \sigma^2\\ \frac{d\overline{xy}}{dt} &= C\overline{x^2} + (A+D)\overline{xy} + B\overline{y^2}\\ \frac{d\overline{y^2}}{dt} &= 2C\overline{xy} + 2D\overline{y^2}\end{aligned}$$

We take $P(\vec{x}, t=0) = \delta x - x_{reset}\delta y - y_{reset}$, so the corresponding initial conditions are $\left[\overline{x}, \overline{y}, \overline{x^2}, \overline{xy}, \overline{y^2}\right]_{t=0} = [x_{reset}, y_{reset}, 0, 0, 0]$ The solutions are:

$$\begin{aligned}\overline{x} &= C_1 e^{\kappa_+ t} + C_2 e^{\kappa_- t}\\ \overline{y} &= C_3 e^{\kappa_+ t} + C_4 e^{\kappa_- t}\end{aligned}$$

$$\begin{aligned}\overline{x^2} =& \frac{\sigma^2}{2(\kappa_+-\kappa_-)^2}[\frac{(\kappa_+-D)^2}{2\kappa_+}(e^{2\kappa_+ t}-1)\\ &+\frac{2BC}{\kappa_++\kappa_-}(e^{(\kappa_++\kappa_-)t}-1)\\ &+\frac{(\kappa_--D)^2}{2\kappa_-}(e^{2\kappa_- t}-1)]\\ \overline{xy} =& \frac{\sigma^2 B}{2(\kappa_+-\kappa_-)^2}[\frac{\kappa_+-D}{2\kappa_+}(e^{2\kappa_+ t}-1)\\ &-\frac{A-D}{\kappa_++\kappa_-}(e^{(\kappa_++\kappa_-)t}-1)\\ &+\frac{\kappa_--D}{2\kappa_-}(e^{2\kappa_- t}-1)]\\ \overline{y^2} =& \frac{\sigma^2 B^2}{2(\kappa_+-\kappa_-)^2}[\frac{1}{2\kappa_-}(e^{2\kappa_+ t}-1)\\ &-\frac{2}{\kappa_++\kappa_-}(e^{(\kappa_++\kappa_-)t}-1)\\ &+\frac{1}{2\kappa_-}(e^{2\kappa_- t}-1)]\end{aligned}$$

where $\kappa_\pm$ and $C_{1,2,3,4}$ are the same as previously defined. Substitution into

$$\begin{aligned}&P(x,y,t)\\ &= \frac{1}{2\pi\sqrt{\overline{x^2}\,\overline{y^2} - \overline{xy}^2}}\\ &exp\left[-\frac{1}{2\left(1-\frac{\overline{xy}^2}{\overline{x^2}\,\overline{y^2}}\right)}\left(\frac{(x-\overline{x})^2}{\overline{x^2}} - \frac{2\overline{xy}(x-\overline{x})(y-\overline{y})}{\overline{x^2}\,\overline{y^2}} + \frac{(y-\overline{y})^2}{\overline{y^2}}\right)\right]\end{aligned}$$

gives the desired result (see Figure 5 for the traces of the two first moments).

IV. NETWORKS OF NEURONS

So far, this model has only focused on a single neuron. To see how a network of connected neurons behave, introduce Δ, the coupling of an action potential from one neuron to all connected neurons. Whenever a neuron reaches the threshold membrane potential, all other connected neurons have their membrane potential is raised by Δ. This is assumed to happen far faster than current can leak out through the membrane, and is therefore taken to be instantaneous. The simplest network is one in which all neurons are connected to all other neurons. The equation 3 then becomes, for the i^{th} neuron:

$$\begin{aligned}x_i(t+dt) =& x_i(t) + \int_t^{t+dt} dt'(Ax_i(t') + By_i(t')) \quad (10)\\ &+\sigma W(t) + \Delta\sum_{j\neq i}\delta(t-t_j) \quad (11)\\ dy_i =& Cx_i + By_i \quad (12)\end{aligned}$$

where t_j represents the times neuron j fires an action potential. The ion pumps of one neuron do not directly

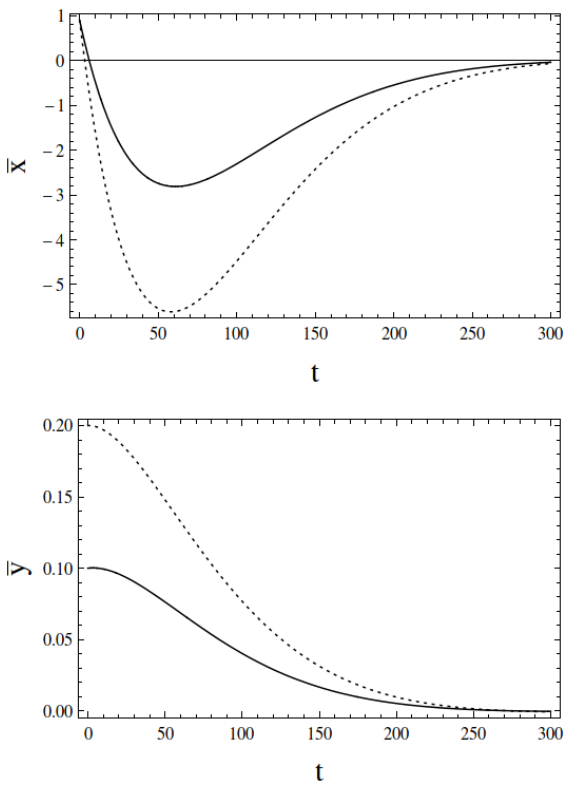

FIG. 5: Time evolution of first moments $\overline{x}(t)$ and $\overline{y}(t)$. The solid line corresponds to initial condition $(x_0, y_0) = (0.9, 0.1)$. The dotted line corresponds to $(x_0, y_0) = (0.9, 0.2)$. *i.e.* the initial conditions are the values for (x, y) immediately after *reset*. As can be seen the time constant of returning to equilibrium 0 is independent of the particular values of y_{reset}, so the overall spiking pattern is independent of such arbitrary choices, as should be the case.

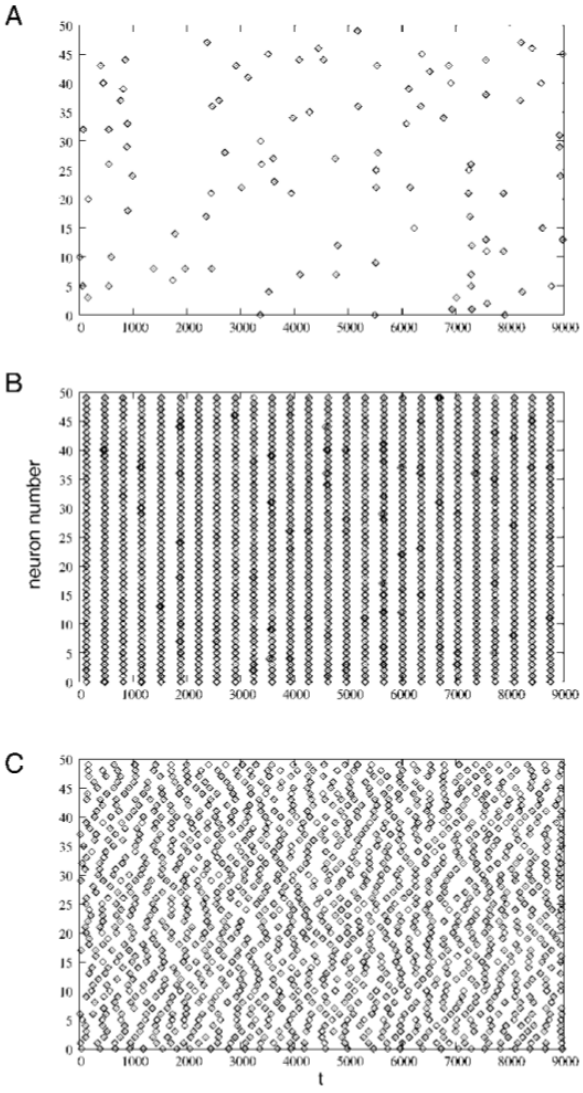

FIG. 6: The plots above are for a network of 50 neurons in which all cells are interconnected. Vertical axis indexes the cells from 1 to 50. Points indicate the times at which a given neuron crosses threshold voltage. $\Delta = 0.06$ is held fixed in this case and σ varied. The three plots show bursting patterns for various noise levels ($\sigma_A = 0.08$, $\sigma_B = 0.12$, $\sigma_C = 0.9$). Synchronization occurs for intermediate noise (*i.e.* graph B). [3]

affect the dynamics of the pumps of another neuron, and thus, 4 remains essentially unchanged ($y \to y_i$). Simulations of this network, at different noise strengths σ show that for "intermediate" noise levels the entire network fires synchronously.

Figure 6 shows qualitatively how the bursting becomes synchronized for mid-strength noise. Alternatively, one can look upon the corresponding ISIH plot (Figure 8), which exhibits the sharpest peaks for intermediate values of σ.

To see how this occurs, consider the state of the network right after the network has fired. For some time afterwards, the membrane potential for any neuron (say the j^{th} neuron) is far less than the threshold so that the dynamics of x_j are dominated by the negative effect of y_j. In this regime, no neurons are likely to cross the threshold, and thus the system can be treated as a set of independent neurons. From the solution of the FPE for an isolated neuron, the probability of x_j reaching the threshold voltage at time t, assuming it starts from the reset value, is:

$$q_j(t) = \int_{x_{thresh}}^{\infty} dx \int_{-\infty}^{\infty} dy P(x, y, t)$$
$$= \int_{x_{thresh}}^{\infty} dx \frac{e^{-(x-\bar{x}(t))^2/(2\sigma_x(t))}}{\sqrt{2\pi\sigma_x(t)}}$$

Plots of this function for various reset conditions and noise levels are shown in Figure 10C.

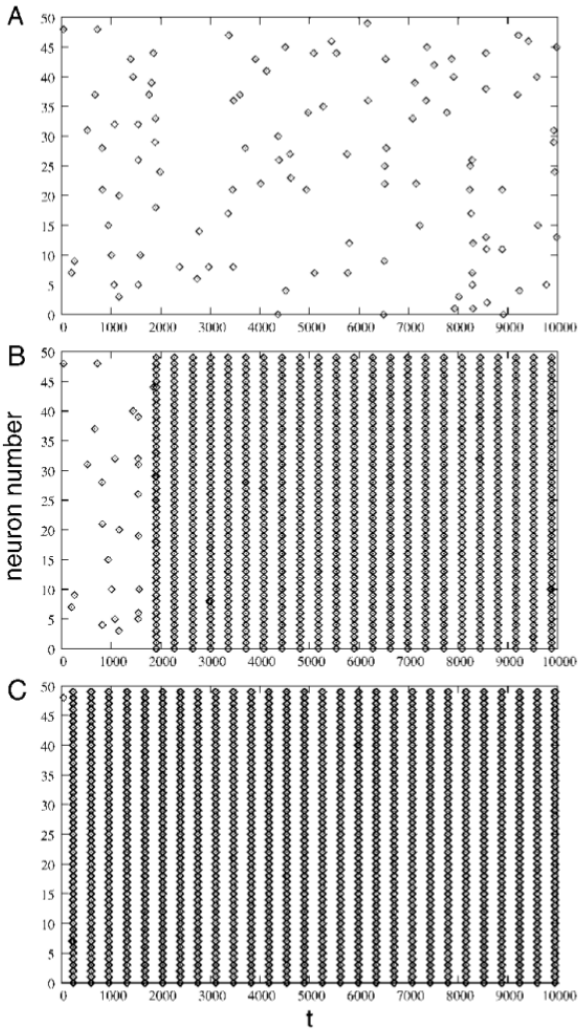

FIG. 7: Bursting patterns for various coupling strengths ($\Delta_A = 0.06$, $\Delta_B = 0.1$, $\Delta_C = 0.2$) with fixed noise $\sigma = 0.08$. For sufficiently large Δ the neurons synchronize with frequency independent of Δ.

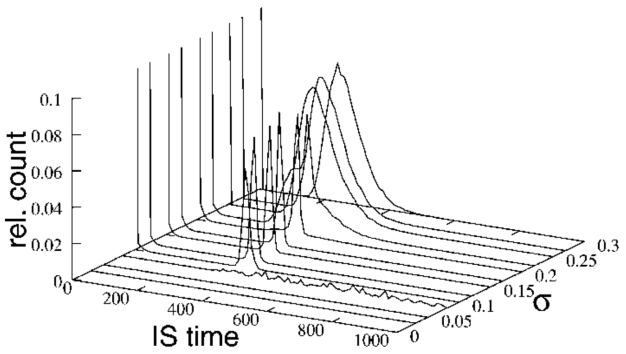

FIG. 8: Inter-spike intervals (with fixed $\Delta = 0.06$) as a function of σ. Synchronization is strongest for intermediate noise levels. [3]

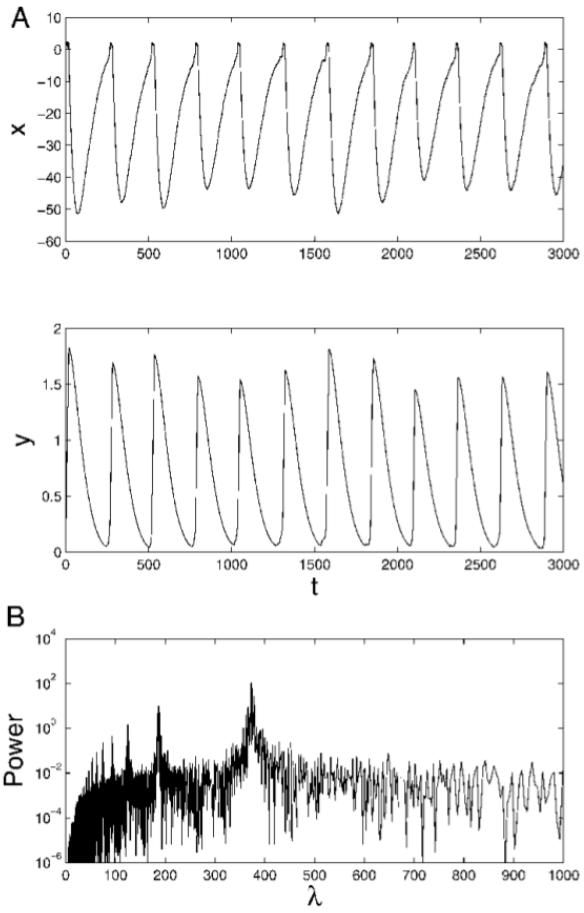

FIG. 9: Averaged traces for a network of 50 neurons with $\sigma = 0.1$ and $\Delta = 0.06$, demonstrating strongly synchronized firing. The third graph is the power spectrum in Fourier space. The strong peak at $\lambda = 366$ is indicative of synchronous behaviour. [3]

Now if a single neuron fires, the x_j of all the other neurons increases by Δ, which corresponds to shifting the mean $\bar{x}$ by Δ in the probability distribution. This will increase the probability that x will be larger than the threshold, and thus increase the chance of another neuron firing. This is shown in Figure 10D, where the probability of firing increases when the mean is shifted by $\Delta = 0.06$, compared to Figure 10C.

This is the chain reaction that leads to a synchronized burst across the entire network; as more and more neurons fire, the probability that other neurons fire increases until all of the neurons have fired. Qualitatively, as the coupling strength Δ increases, the more synchronized the network becomes. If the coupling strength is infinite, a single action potential will cause the entire network to fire. If the coupling strength is zero, all neuron bursts are independent and unsynchronized. Thus, the

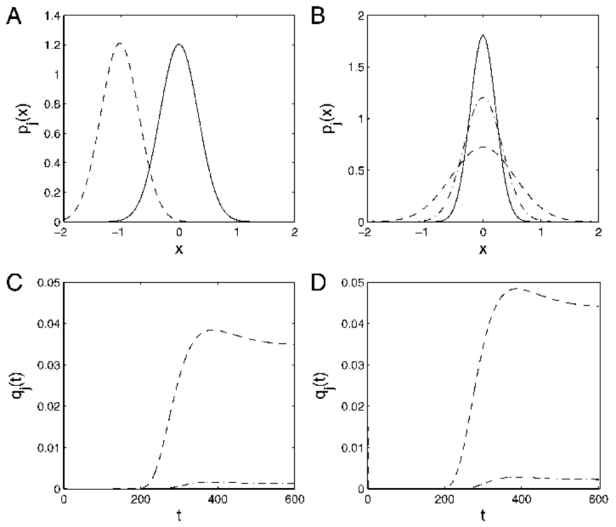

FIG. 10: For the plots above, initial conditions are always taken to be reset values $(x_0, y_0) = 0.9, 0.2$ **(A)** Marginal density for x_j, $p_j(x,t) \equiv \int_{-\infty}^{\infty} dy P(x,y,t)$, for $\sigma = 0.12$ at $t = 200, 330$. **(B)** $p_j(x,t)$ at $t = 330$ for $\sigma = 0.08(solid), 0.12(dash-dotted), 0.2(dashed)$ *i.e.* from "*sharpest* to *flattest*. **(C)** $q_j(t)$ corresponding to the $\sigma = 0.12, 0.2$ curves of sub-figure B. **(D)** $q_j(t)$ corresponding to the curves of sub-figure B supposing the means in B had all been shifted by coupling strength Δ. [3]

synchronization of the network increases with the coupling strength Δ.

The reason why synchronization is not present at low noise levels is apparent from a graph of the probability distribution $\int_{-\infty}^{\infty} dy P(x,y,t)$ in Figure 10B. At low levels of noise, the variance is low, so any neuron reaching the threshold voltage is unlikely, even when kicked by other neurons. Of course, with a strong enough coupling, one would eventually see synchronous bursting; even one neuron bursting could raise the membrane potential of the other neurons enough to initiate a cascade of action potentials, as in Figure 7.

The disappearance of synchronized bursting at high noise levels of noise is a more subtle point. Bursting is synchronized because, after each burst, the dynamics of x are dominated by the inhibition of the voltage from the ion channels, $-By$. Thus, the mean neuron potential is far from the threshold and bursting is unlikely. However, for sufficiently strong noise ($\sigma \sim \mathcal{O}(By_{reset})$), this is not true. In this regime, the inhibitory effect of the open ion channels does not dominate over the noise, and the probability of bursting is not negligible. Thus, synchronization is lost because even if the first bursting event occurred across the entire network, the neurons are not inhibited from firing again, and will fire randomly, destroying the coherence observed at lower noise levels.

This resonant integrate-and-fire model of neural networks shows several properties seen in several other more detailed models, particularly the Hindmarsh-Rose model. Although simpler than the Hindmarsh-Rose model, it displays similar sub-threshold and burst behaviour. Analysing the effect of stochastic noise on a fully connected neural network led to the observation that the noise could induce synchronized, periodic bursting throughout the network. This effect is the result of the interplay between the drainage of charge through ion channels, neuron-neuron coupling, and stochastic noise. In particular, the synchronization appears to have a "resonant" noise level; synchronization appears only in a narrow range of noise strengths σ, for a given neuron-neuron coupling strength.

[1–3]

[1] Daniel Arovas. *Lecture Notes on Nonequilibrium Statistical Physics*. UCSD, La Jolla, 2013.

[2] Crispin Gardiner. *Stochastic Methods*. Springer, Berlin, 2009.

[3] Rachel Kuske Stefan Reinker, Yue-Xian Li. Noise-induced coherence and network oscillations in a reduced bursting model. *Bulletin of Mathematical Biology*, 68:1401–1427, 2006.